

## Structural Transformations in Thin Ge<sub>2</sub>Sb<sub>2</sub>Te<sub>5</sub> Films

S. A. Kozyukhin<sup>a</sup>, A. A. Sherchenkov<sup>b</sup>, E. V. Gorshkova<sup>b</sup>, V. Kh. Kudoyarova<sup>c</sup>, and A. I. Varginin<sup>a</sup>

<sup>a</sup> Kurnakov Institute of General and Inorganic Chemistry, Russian Academy of Sciences,  
Leninskii pr. 31, Moscow, 119991 Russia

<sup>b</sup> Moscow Institute of Electronic Technology (Technical University), proezd 4806 5, Zelenograd, Moscow, 124498 Russia

<sup>c</sup> Ioffe Physicotechnical Institute, Russian Academy of Sciences, Politekhnicheskaya ul. 26, St. Petersburg, 194021 Russia

e-mail: sergkoz@hotmail.ru

Received June 16, 2008

**Abstract**—Structural transformations in thin Ge<sub>2</sub>Sb<sub>2</sub>Te<sub>5</sub> films for phase-change memory applications have been studied by differential scanning calorimetry. As-grown, amorphous films have been shown to undergo structural transitions to a cubic and then to a hexagonal phase. A reproducible endothermic peak has been detected, which had not been reported earlier. A mechanism for the underlying process has been proposed.

**DOI:** 10.1134/S0020168509040050

### INTRODUCTION

Thin-film materials based on chemical compounds of the pseudobinary system GeTe–Sb<sub>2</sub>Te<sub>3</sub> have been intensely studied in the past decade as attractive media for phase-change memory applications, in particular for DVD-RW optical disks and nonvolatile memory cells [1–3]. Such devices take advantage of reversible rapid amorphous  $\longleftrightarrow$  crystalline phase transitions that occur at the nanoscale in response to low-energy external stimuli (light or electrical pulses). The effects underlying such behavior in semiconducting chalcogenide glasses were first observed by Lebedev and Kolomiets [4] and Ovshinsky [5], which allowed the first Ge–Te memory arrays to be presented in the early 1970s [6]. In spite of the intense interest in Ge–Sb–Te (GST) materials and the obvious commercial success of phase-change technology, many issues pertaining to the nature of these materials have not yet been addressed in sufficient detail. These are primarily the nature of the amorphous state and the mechanisms of electronic switching and subsequent crystallization.

One of the most attractive and best studied phase-change memory materials in commercial use is Ge<sub>2</sub>Sb<sub>2</sub>Te<sub>5</sub> (GST225). Because quantitative evaluation of crystallization kinetics requires knowledge of the fundamental thermal properties of both the crystalline and amorphous phases (melting, crystallization, and softening temperatures of the glass, heat effects, and others), one of the most informative experimental methods is thermal analysis, in particular differential scanning calorimetry (DSC). A detailed analysis of the literature has shown, first, that not much information is available and, second, that published data, though consistent on the whole, often differ in important details [7–10]. We think that this is related not only to the complex structure of crystalline GST225 and related thin

films but also to the fact that amorphous layers produced by different techniques and in different laboratories vary in structure. Nevertheless, summarizing the results of the above-mentioned studies, we can pinpoint several typical features:

1. In none of those studies was any heat effect related to the softening temperature of the amorphous phase,  $T_g$ , detected experimentally.

2. Slow heating of amorphous GST225 films results in broad, composite exothermic peaks corresponding to amorphous  $\longrightarrow$  cubic (crystalline) and cubic  $\longrightarrow$  hexagonal phase transitions.

3. No exothermic events occur at temperatures above 300°C; at  $\sim$ 620°C, there is an endothermic peak corresponding to the melting point,  $T_m$ .

At the same time, there are reports that structural transformations are possible in the temperature range 300–500°C, which requires further research.

In this paper, we present a DSC study of thin GST225 films as are used in phase-change memory cells.

### EXPERIMENTAL

Thin-film Ge<sub>2</sub>Sb<sub>2</sub>Te<sub>5</sub> structures were grown on (100) single-crystal Si substrates by thermal evaporation in a vacuum chamber at a residual pressure of  $10^{-4}$  Pa. The maximum temperature of the evaporation source was 630°C, and the substrate temperature was no higher than 50°C, which enabled the preparation of amorphous films. Under the conditions of this study, the growth rate of the films was about 3 nm/s. The source material used was polycrystalline Ge<sub>2</sub>Sb<sub>2</sub>Te<sub>5</sub> synthesized from semiconductor-grade elements as described elsewhere [11]. The phase composition of the films was deter-

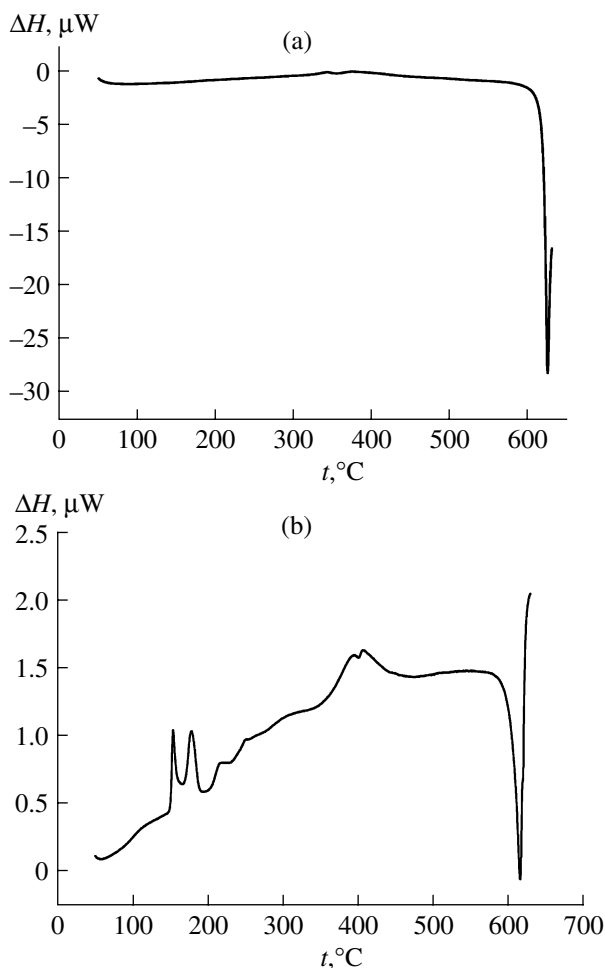


**Fig. 1.** DSC curves of  $\text{Ge}_2\text{Sb}_2\text{Te}_5$ : (a) parent polycrystalline material, (b) thin-film amorphous sample.

mined by X-ray diffraction (DRON-3 diffractometer) or inferred from resistivity measurements (Keithley 6485 picoammeter). The room-temperature resistivity of the amorphous films was approximately four orders of magnitude higher than that of the crystalline films. The thickness of the films was  $\approx 900$  nm as determined by atomic force microscopy (NT-MDT Solver Pro scanning probe microscope).

The chemical composition of the amorphous films was determined by two techniques: Rutherford backscattering (RBS) spectroscopy (1-MeV deuteron backscattering) and X-ray fluorescence analysis. That antimony and tellurium are neighbors in the Periodic Table creates some difficulties in quantitative spectral analysis. For this reason, only the  $\frac{\text{Ge}}{\text{Sb} + \text{Te}}$  ratio in the  $\text{Ge}_2\text{Sb}_2\text{Te}_5$  thin films was determined by RBS, because we failed to resolve the scattered particle signals corresponding to antimony and tellurium. The experimentally determined ratio,  $[\text{Ge}_{0.31}(\text{Sb} + \text{Te})_1]$ , agrees with the  $\text{Ge}_2\text{Sb}_2\text{Te}_5$  stoichiometry,  $[\text{Ge}_{0.29}(\text{Sb} + \text{Te})_1]$ , within

the accuracy limits of the technique ( $\pm 5\%$ ). An attempt was made to determine the Sb : Te ratio in the films by X-ray fluorescence analysis ( $^{55}\text{Fe}$  X-ray source, excitation at 5.9 and 6.49 keV, 100-eV resolution of the Si detector). Because of the significant overlap of the Sb *L* and Te *L* peaks, the accuracy of this technique proved substantially lower in comparison with RBS, and we were able to conclude only that the antimony : tellurium ratio in the films was in semiquantitative agreement with that in the parent compound.

Calorimetric scans were performed with a Shimadzu DSC-50. The required amount of amorphous material (about 2–4 mg) was collected by scraping the deposit off the silicon substrate. The sensitivity of the instrument was  $10 \mu\text{W}$ , and the temperature range studied was 20 to  $630^\circ\text{C}$ . The sample was enclosed in an Al crucible and heated at a rate  $q = 5$  to  $70^\circ\text{C}/\text{min}$ .

## RESULTS AND DISCUSSION

Figure 1 shows DSC curves of polycrystalline  $\text{Ge}_2\text{Sb}_2\text{Te}_5$  and a thin amorphous film of the same composition. The curve of the polycrystalline material is featureless between room temperature and  $595^\circ\text{C}$  (Fig. 1a). At  $595^\circ\text{C}$ , there is the onset of the endothermic peak corresponding to the beginning of the liquidus range. The maximum peak temperature, corresponding to the melting point, is  $t_m = 624.6^\circ\text{C}$ . The DSC curves of the as-prepared thin-film samples showed a number of thermal events, and the melting endotherm occurred at a lower temperature:  $t_m = 616.4^\circ\text{C}$  (Fig. 1b).

Figure 2 shows DSC curves of the amorphous material at different heating rates. The shape of the curves varies systematically with heating rate. The curves can be divided into two distinct groups: those obtained at  $q_1 = 5\text{--}15^\circ\text{C}/\text{min}$  (Fig. 2a) and  $q_2 = 40\text{--}70^\circ\text{C}/\text{min}$  (Fig. 2b). The curve obtained at  $q = 20^\circ\text{C}/\text{min}$  is intermediate in shape. The following features are common to all of the curves:

1. The heat effect due to the softening of the amorphous phase was not detected at the heating rates used.
2. In the range  $\Delta t = 145\text{--}190^\circ\text{C}$ , the curves show a large, broad, composite exotherm. According to earlier results [8–10], this exotherm is due to the transition of the amorphous phase to the NaCl (fcc) structure of the low-temperature, metastable phase of  $\text{Ge}_2\text{Sb}_2\text{Te}_5$  [12]. Note that it is this transition which is critical to the performance of phase-change memory cells.
3. The exotherm in the range  $\Delta t = 205\text{--}230^\circ\text{C}$  is substantially smaller and is due to the transition of the metastable, cubic phase (fcc) to a stable hexagonal phase (hcp).
4. The broad exotherm in the range  $\Delta t = 250\text{--}330^\circ\text{C}$  is present in all of the curves, in contrast to earlier reported results.

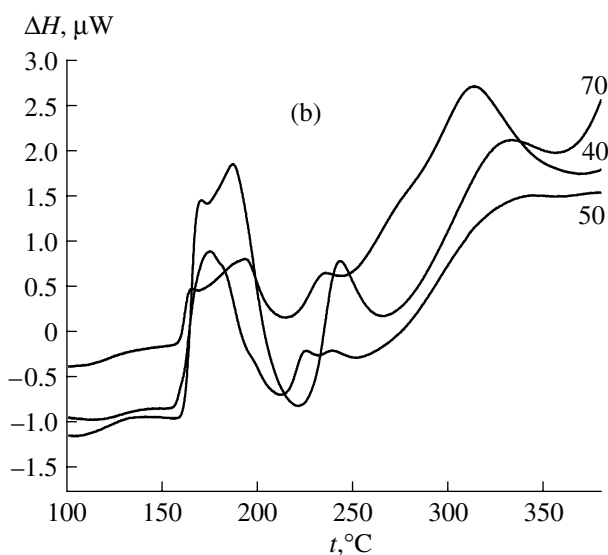
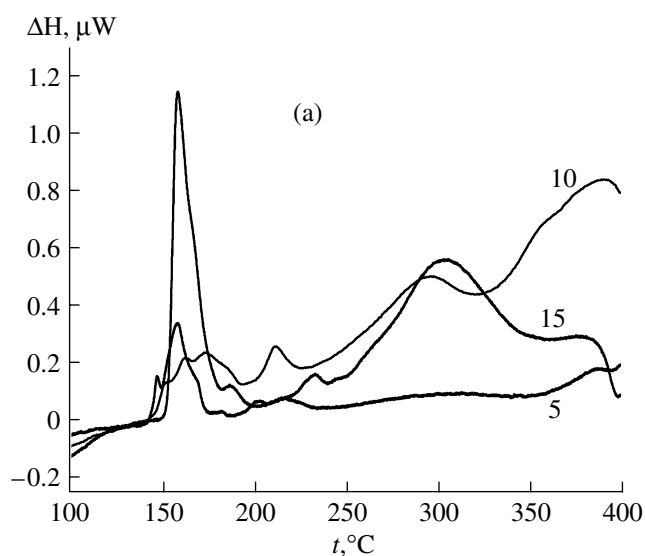


**Fig. 2.** DSC curves of thin-film amorphous  $\text{Ge}_2\text{Sb}_2\text{Te}_5$  at different heating rates (indicated by the numbers at the curves).

5. There is an endothermic peak in the range  $\Delta t = 390\text{--}415^\circ\text{C}$ , which also has not been reported in the literature.

Measurements at a slower heating rate provide more detailed information. With increasing heating rate, the thermal events shift to higher temperatures. During a second DSC scan of the sample prepared from a thin amorphous film, most of the observed peaks disappear, as expected, except for the peak indicated in paragraph 5.

Table 1 compares the present experimental data and results obtained by other groups at comparable heating rates. Note the data reported by Kalb et al. [8]: for the composition in question, they identified  $t_g$  with the crystallization onset at a fast heating rate  $q = 80^\circ\text{C}/\text{min}$ .

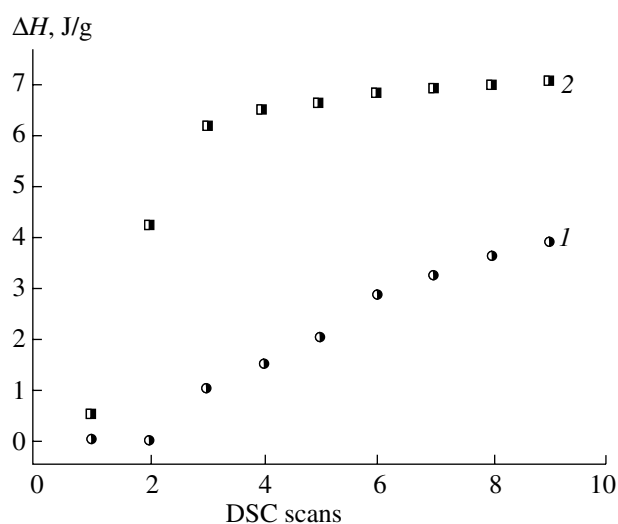


**Fig. 3.** Heat effect  $\Delta H$  associated with the endotherm in the range  $390\text{--}415^\circ\text{C}$  as a function of the number of DSC scans: (1) parent polycrystalline material, (2) as-prepared thin-film amorphous sample.

Thus, our DSC data indicate that the parent polycrystalline material is in an equilibrium state and undergoes no polymorphic transformations. At the same time, the amorphous films are out of equilibrium, with metastable states.

DSC measurements on an initially amorphous sample showed that the heat effect associated with the endothermic process in the range  $390\text{--}415^\circ\text{C}$  increased in three consecutive DSC scans and then saturated. At the same time, for the parent crystalline material this peak became discernible only after the third scan and then increased in each scan. Figure 3 presents experimental data that illustrate the dynamics of changes in the height of this peak.

After such a series of DSC scans, visual examination of the material obtained from a thin-film sample in an aluminum crucible showed that the material experienced only sintering, with no indication of partial melting or reaction with the crucible. This may be interpreted as evidence that no precipitation or melting of any phases occurred in the temperature range studied.

DSC measurements at different heating rates allowed us to use Kissinger analysis in order to evaluate the activation energy for the observed thermal events [13]. Figure 4 shows the Kissinger plots obtained, and Table 2 lists the corresponding activation energies.

The activation energy we obtained for the transition of the amorphous phase to the NaCl (fcc) structure is somewhat lower than those reported in the literature, which can be accounted for by the difference in the techniques used to prepare thin films and evaluate the activation energy. The difference in activation energy is more significant for the  $\text{fcc} \rightarrow \text{hcp}$  phase transition, which indicates that the process is of a complex nature and that one should take into account the approach used

**Table 1.** DSC data for amorphous GST225 films

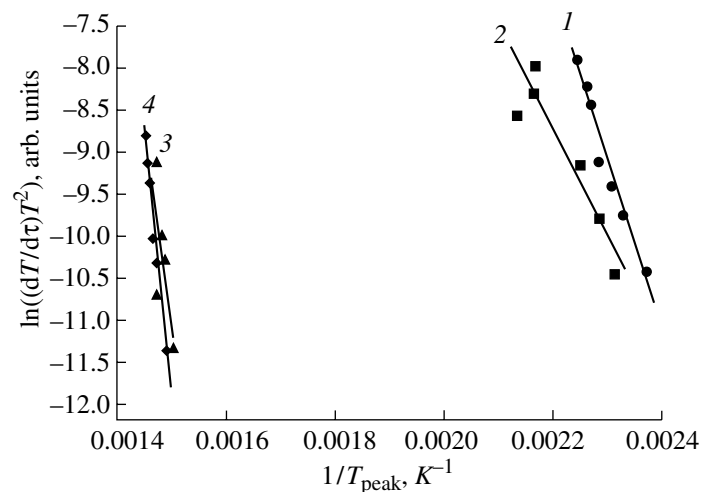
Heating rate, °C/min	$t_g$ , °C	$t_x$ , °C	Phase transitions	Source
5	–	101–163°ë ( $t_x > 155^\circ\text{C}$ ) >200°C	Amorphous $\longrightarrow$ cubic ( <i>fcc</i> ) Cubic $\longrightarrow$ hexagonal ( <i>hcp</i> )	[8]
80	173°ë	173°ë		
10	–	172.7°ë 365.3°ë	Amorphous $\longrightarrow$ cubic ( <i>fcc</i> ) Cubic $\longrightarrow$ hexagonal ( <i>hcp</i> )	[9]
10	–	160°ë		[10]
10	–	170°ë 217°ë	Amorphous $\longrightarrow$ cubic ( <i>fcc</i> ) Cubic $\longrightarrow$ hexagonal ( <i>hcp</i> )	This work
70	–	185°ë		

**Table 2.** DSC results in comparison with earlier data

Sample	Peak position, °C	Type	Transition	Activation energy, eV
Source material	390–415	Endo		5.79
Thin films	145–190	Exo	Amorphous $\longrightarrow$ cubic ( <i>fcc</i> )	1.77
	$t_x > 155$ [8]			2.23 [7]
	$t_x > 172.7$ [9]			
	$t_x > 160$ [10]			
	205–230	Exo	Cubic $\longrightarrow$ hexagonal ( <i>hcp</i> )	1.22 3.64 $\pm$ 0.19 [18]
	$t_x > 200$ [8]			
	$t_x > 365.3$ [9]			
	250–330	Exo		1.67
	390–415	Endo		5.57

to evaluate this parameter (Friedrich et al. [14] extracted it from electrical conductivity data). The activation energy for the endothermic process in the range 390–415°C proved markedly higher than those for the

other thermal events and changed little in going from the source material to thin-film samples (Fig. 4, curves 3, 4). The high activation energy of this process indicates that its rate is rather slow.

**Fig. 4.** Kissinger plots for  $\text{Ge}_2\text{Sb}_2\text{Te}_5$ : (1) amorphous  $\longrightarrow$  cubic (crystalline) phase transition, (2) cubic  $\longrightarrow$  hexagonal phase transition, (3) endothermic process in the amorphous thin-film material, (4) endothermic process in the parent polycrystalline material.

Thus, the present experimental data attest to an endothermic process in the range 390–415°C, which was not detected in early DSC studies of GST225. Note, however, that a thermal event near 400°C was observed in a few very recent experimental studies. In particular, based on electron microscopy results Chen et al. [15] attributed the endothermic peak at 400°C to tellurium agglomeration.

Nevertheless, the origin of this endotherm is still poorly understood. Certain assumptions as to the underlying mechanism can be made based on published structural data. Both the amorphous and metastable cubic phases of GST225 are known to contain structural elements missing in the hexagonal phase, e.g., vacancies ( $\approx 20\%$ ) in the Ge/Sb layers, three-coordinate Te atoms ( $\approx 17\%$ ), and structural units corresponding to the Ge<sub>17</sub>Te<sub>83</sub> eutectic in the GeTe–Te system [16–19]. There are grounds to believe that such defects play a key role in the structural transformations in question and are responsible for the endotherm near 400°C. The tellurium agglomeration observed by Chen et al. [15] can then be correlated with the formation of structural units corresponding to the Ge<sub>17</sub>Te<sub>83</sub> eutectic. The important role of Ge–Te structural units in GST and phase-change memory effects was pointed out earlier [17, 18].

#### ACKNOWLEDGMENTS

This work was supported by the Russian Foundation for Basic Research, project no. 08-03-00651.

#### REFERENCES

1. Neale, R., Amorphous Non-Volatile Memory: The Past and the Future, *Electron. Eng.*, April 2001, pp. 61–74.
2. Hudgens, S. and Johnson, B., Overview of Phase-Change Chalcogenide Nonvolatile Memory Technology, *MRS Bull.*, 2004, vol. 29, no. 11, pp. 829–832.
3. Lacaíta, A.L., Phase-Change Memories: State-of-the-Art, Challenges and Perspectives, *Solid-State Electron.*, 2006, vol. 50, pp. 24–31.
4. Lebedev, E.A. and Kolomiets, B.T., *Radiotekh. Elektron.* (Moscow), 1963, vol. 8, pp. 2037–2041.
5. Ovshinsky, S.R., Reversible Electrical Switching Phenomena in Disordered Structures, *Phys. Rev. Lett.*, 1968, vol. 21, no. 20, pp. 1450–1453.
6. Evans, E.J., Helbes, J.H., and Ovshinsky, S.R., Reversible Conductivity Transformations in Chalcogenide Alloy Films, *J. Non-Cryst. Solids*, 1970, vol. 2, pp. 334–346.
7. Yamada, N., Ohno, E., Nishiuchi, K., et al., Rapid-Phase Transitions of GeTe–Sb<sub>2</sub>Te<sub>3</sub> Pseudobinary Amorphous Thin Films for An Optical Disk Memory, *J. Appl. Phys.*, 1991, vol. 69, pp. 2849–2856.
8. Kalb, J., Spaepen, F., and Wutting, M., Calorimetric Measurements of Phase Transformations in Thin Films of Amorphous Te Alloys Used for Optical Data Storage, *J. Appl. Phys.*, 2003, vol. 95, no. 5, pp. 2389–2393.
9. Zhang, T., Liu, B., Song, Z.-T., et al., Phase Transition Phenomena in Ultra-Thin Ge<sub>2</sub>Sb<sub>2</sub>Te<sub>5</sub> Film, *Chin. Phys. Lett.*, 2005, vol. 22, no. 7, pp. 1803–1805.
10. Seo, H., Jenó, T.-H., Park, J.-W., et al., Investigation of Crystallization Behavior of Sputter-Deposited Nitrogen-Doped Amorphous Ge<sub>2</sub>Sb<sub>2</sub>Te<sub>5</sub> Thin Films, *Jpn. J. Appl. Phys.*, 2000, vol. 39, pp. 745–751.
11. Abrikosov, N.Kh. and Danilova-Dobryakova, G.T., Sb<sub>2</sub>Te<sub>3</sub>–GeTe Phase Diagram, *Izv. Akad. Nauk SSSR, Neorg. Mater.*, 1965, vol. 1, no. 2, pp. 204–208.
12. Kosyakov, V.I., Shestakov, V.A., Shelimova, L.E., et al., Topological Characterization of the Ge–Sb–Te Phase Diagram, *Neorg. Mater.*, 2000, vol. 36, no. 10, pp. 1196–1209 [*Inorg. Mater.* (Engl. Transl.), vol. 36, no. 18, pp. 1004–1017].
13. Kissinger, H.E., Reaction Kinetics in Differential Thermal Analysis, *Anal. Chem.*, 1957, vol. 29, pp. 1702–1706.
14. Friedrich, I., Weidenhof, V., Nijoroge, W., et al., Structural Transformations of Ge<sub>2</sub>Sb<sub>2</sub>Te<sub>5</sub> Films Studied by Electrical Resistance Measurements, *J. Appl. Phys.*, 2000, vol. 87, no. 9, pp. 4130–4134.
15. Chen, K.N. Cabrai, C., Jr., and Krusin-Elbaum, L., Segregation of Te and Irreversible Modification in Ge<sub>2</sub>Sb<sub>2</sub>Te<sub>5</sub> Phase Change Material, *E-MRS Spring Meet.*, 2008, H11.
16. Petrov, I.I., Imamov, R.M., and Pinsker, G.Z., Structures of Ge<sub>2</sub>Sb<sub>2</sub>Te<sub>5</sub> and GeSb<sub>4</sub>Te<sub>7</sub> Determined by Electron Diffraction, *Kristallografiya*, 1968, vol. 13, no. 3, pp. 417–421.
17. Matsunaga, T., Yamada, N., and Kubota Yosh, Structures of Stable and Metastable Ge<sub>2</sub>Sb<sub>2</sub>Te<sub>5</sub>, an Intermetallic Compound in Ge–Te–Sb<sub>2</sub>Te<sub>3</sub> Pseudo-Binary System, *Acta Crystallogr., Sect. B: Struct. Sci.*, 2004, vol. 60, pp. 685–691.
18. Paesler, M.A., Baker, D.A., Lucovsky, G., et al., Bond Constraint Theory and EXAFS Studies of Local Bonding Structures of Ge<sub>2</sub>Sb<sub>2</sub>Te<sub>4</sub>, Ge<sub>2</sub>Sb<sub>2</sub>Te<sub>5</sub> and Ge<sub>2</sub>Sb<sub>2</sub>Te<sub>7</sub>, *J. Opt. Adv. Mater.*, 2007, vol. 9, no. 10, pp. 2996–3001.
19. Hansen, M. and Anderko, K., *Constitution of Binary Alloys*, New York: McGraw-Hill, 1958, 2nd ed. Translated under the title *Struktury dvoynykh splavov*, Moscow: Metallurgizdat, 1962, vol. 2, pp. 824–825.

SPELL: OK